

Knowledge Distillation Meets Open-Set Semi-Supervised Learning

Jing Yang, Xiatian Zhu, Adrian Bulat, Brais Martinez, Georgios Tzimiropoulos

Abstract—Existing knowledge distillation methods mostly focus on distillation of teacher’s prediction and intermediate activation. However, the structured representation, which arguably is one of the most critical ingredients of deep models, is largely overlooked. In this work, we propose a novel *Semantic Representational Distillation (SRD)* method dedicated for distilling representational knowledge semantically from a pretrained teacher to a target student. The key idea is that we leverage the teacher’s classifier as a semantic critic for evaluating the representations of both teacher and student and distilling the semantic knowledge with high-order structured information over all feature dimensions. This is accomplished by introducing a notion of cross-network logit computed through passing student’s representation into teacher’s classifier. Further, considering the set of seen classes as a basis for the semantic space in a combinatorial perspective, we scale SRD to unseen classes for enabling effective exploitation of largely available, arbitrary unlabeled training data. At the problem level, this establishes an interesting connection between knowledge distillation with open-set semi-supervised learning (SSL). Extensive experiments show that our SRD outperforms significantly previous state-of-the-art knowledge distillation methods on both coarse object classification and fine face recognition tasks, as well as less studied yet practically crucial binary network distillation. Under more realistic open-set SSL settings we introduce, we reveal that knowledge distillation is generally more effective than existing Out-Of-Distribution (OOD) sample detection, and our proposed SRD is superior over both previous distillation and SSL competitors. The source code is available at https://github.com/jingyang2017/SRD_oss1.

Index Terms—Knowledge distillation, Structured representational knowledge, Open-set semi-supervised learning, Out-of-distribution.

1 INTRODUCTION

OPTIMIZING lightweight Convolutional Neural Networks (CNNs) to be highly performing is critical, *e.g.*, enabling the developments on resource-limited platforms such as mobile devices. To that end, different model compression approaches have been extensively investigated, including network pruning [1], [2], network quantization [3], [4], neural architecture search [5], [6], and knowledge distillation [7], [8]. In particular, knowledge distillation aims to transfer the knowledge from a stronger network (*i.e.*, the teacher) to another (*i.e.*, the student). Typically, the teacher is a high-capacity model or an ensemble capable of achieving stronger performance, while the student is a compact model with much fewer parameters and requiring much less computation. The *objective* is to facilitate the optimization of the student by leveraging the teacher’s capacity. A general rationale behind distillation can be explained from an optimization perspective that higher-capacity models are able to seek for better local minima thanks to over-parameterization [9], [10].

Existing knowledge distillation methods start with transferring classification predictions [7] and intermediate repre-

sentations (*e.g.*, feature tensors [11] and attention maps [8]). However, they suffer from a limitation of distilling *structured* representational knowledge including the latent complex interdependencies and correlations between different dimensions. This is because their objective formulations typically treat all the feature or prediction dimensions *independently*. Motivated by this analysis, a representation distillation method [12] is recently developed by contrastive learning [13], [14]. The concrete idea is to maximize the representation’s mutual information across the teacher and student via contrastive learning. Despite a principled solution following seminal information theory [15], this method is limited in high-level semantics perception and distillation. Because the teacher’s classifier, that maps the feature representation to the semantic class space, is totally ignored during distillation. Further, contrastive learning often requires a large number of training samples in loss computation, meaning a need of resource demanding large mini-batch or complex remedy (*e.g.*, using a memory bank).

To overcome the aforementioned limitations, in this work a novel *Semantic Representational Distillation (SRD)* is introduced. Our key idea is to leverage the pretrained teacher’s classifier as a *semantic critic* for guiding representational distillation in a classification-aware manner. Concretely, we introduce a notion of cross-network logit, obtained by feeding the student’s representation to the teacher’s classifier. Subject to the teacher and student sharing the same input, aligning the cross-network logit with the teacher’s counterpart can then enable the distillation of high-order semantic correlations among feature dimensions, *i.e.*, semantic distillation of representation. Further, we extend the proposed SRD to open-set semi-supervised learning (SSL) by exploiting unconstrained unlabeled data

- Jing Yang is with University of Nottingham, Nottingham, UK. Email: y.jing2016@gmail.com.
- Xiatian Zhu is with Samsung AI Centre, Cambridge, UK, and Surrey Institute for People-Centred Artificial Intelligence, and the Centre for Vision, Speech and Signal Processing (CVSSP), University of Surrey, Guildford, UK. Email: xiatian.zhu@surrey.ac.uk.
- Adrian Bulat and Brais Martinez are with Samsung AI Centre, Cambridge, UK. Email: adrian@adrianbulat.com, brais.a@samsung.com.
- Georgios Tzimiropoulos is with Samsung AI Centre, Cambridge, UK, and Queen Mary University London, London, UK. Email: g.tzimiropoulos@qmul.ac.uk.

from arbitrary classes. This is motivated by a perspective that seen classes of labeled training data can be regarded *collectively* as a basis of the semantic space in the linear algebra theory – any unseen class can be approximated by a specific combination of seen classes. This favorably breaks the restriction to seen classes in model optimization, resulting in a new approach to solving the challenging open-set SSL problem.

Our **contributions** are three-fold: **(I)** We propose a simple yet effective *Semantic Representational Distillation* (SRD) method with a focus on structured representation optimization via semantic knowledge distillation. This is realized by taking the teacher’s classifier as a semantic critic used for evaluating both teacher and student’s representation in terms of their classification performance and ability. **(II)** We connect semantic distillation with open-set semi-supervised learning based on an idea that seen classes can be used as a basis of the semantic space. **(III)** Extensive experiments show that the proposed SRD method can train more generalizable student models than the state-of-the-art distillation methods across a variety of network architectures (*e.g.*, Wide ResNets, ResNets, and MobileNets) and recognition tasks (*e.g.*, coarse-grained object classification and fine-grained face recognition, real and binary network distillation). Compared to previous open-set SSL works, we further introduce more realistic experiment settings characterized by more classes and unlabeled data with different distributions, as well as less common classes between labeled and unlabeled sets. Critically, our experiments reveal that knowledge distillation turns out to be a more effective strategy than previously often adopted Out-Of-Distribution (OOD) detection (Table 10 *vs.* Table 11), and our SRD outperforms both state-of-the-art distillation and SSL methods, often by a large margin. On the other hand, it is also shown that OOD detection brings very marginal benefits to knowledge distillation methods (Table 12).

This is an extension of our preliminary ICLR 2021 work [16]. We further make the following significant contributions: **(1)** Extending our method in general knowledge distillation to open-set semi-supervised learning, two previously independently investigated fields. **(2)** Analyzing the limitations of existing open-set SSL settings and introducing more realistic ones with less constrained unlabeled data such as less class overlap between labeled and unlabeled sets. **(3)** Evaluating and comparing comprehensively both knowledge distillation and open-set SSL methods with new findings and insights in tackling more unconstrained unlabeled data. **(4)** To show the generality of our approach, we evaluate on a diverse range of problems with varying underlying characteristics, such as coarse-grained object classification tasks and fine-grained face recognition distillation.

2 RELATED WORK

2.1 Knowledge Distillation

Knowledge distillation is an effective approach to optimizing low-capacity networks with extensive studies in image classification [7], [11], [8], [17], [18], [19], [20], [21], [22], [23], [24], [25], [26], [27], [28], [29], [30]. Existing distillation methods can be generally divided into two categories: isolated knowledge based and relational knowledge based.

Isolated knowledge based methods: The seminal work in Hinton et al. [7] popularized the research on knowledge distillation by simply distilling the teacher’s classification outputs (*i.e.*, the knowledge). Compared to one-hot class label representation, this knowledge is semantically richer due to involving underlying inter-class similarity information. Soon after, intermediate teacher representations such as feature tensors [11] are also leveraged for richer distillation. However, matching the whole feature tensors is not necessarily viable in certain circumstances due to the capacity gap between the teacher and student, even adversely affecting the performance and convergence of the student. As an efficient remedy, Attention Transfer (AT) [8] might be more achievable as the feature attention maps (*i.e.*, a summary of all the feature channels) represent a more flexible knowledge to be learned. The following extended AT based on the maximum mean discrepancy of the activations [17] shares the same spirit. Interestingly, Cho *et al.* [26] reveal that very highly strong networks would be “too good” to be effective teachers. To mitigate this issue, they early stop the teacher’s training. Later on, Heo *et al.* [30] study the effect of distillation location within the network, along with margin ReLU and a specifically designed distance function for maximizing positive knowledge transfer. More recently, Passalis *et al.* [31] leverage the previously ignored information plasticity by exploiting information flow through teacher’s layers.

Relational knowledge based methods: Another line of knowledge distillation methods instead explore relational knowledge. For example, Yim *et al.* [18] distil the feature correlation by aligning the layer-wise Gram matrix of feature representations across the teacher and student. A clear limitation of this method is at a high computational cost. This could be alleviated to some extent by compressing the feature maps using singular value decomposition [21]. Park *et al.* [27] consider both distance-wise and angle-wise relations of each embedded feature vector. This idea is subsequently extended by [25] for better capturing the correlation between multiple instances with Taylor series expansion, and by [28] for modeling the feature space transformation across layers via a graph with the instance feature and relationship as vertexes and edges. Inspired by an observation that semantically similar samples should give similar activation patterns, Tung *et al.* [22] introduce an idea of similarity-preserving knowledge distillation *w.r.t.* the generation of either similar or dissimilar activations. Besides, Jain *et al.* [32] exploit the relational knowledge *w.r.t.* a quantized visual word space during distillation. For capturing more detailed and fine-grained information, Li *et al.* [33] employ the relationship among local regions in the feature space. In order to distil richer representational knowledge from the teacher, Tian *et al.* [12] maximize the representation’s mutual information between the teacher and student. Whilst sharing a similar objective, in this work we instead correlate the teacher’s and student’s representations via considering the pretrained teacher’s classifier as a semantic critic. Despite its simplicity, we show that our method is superior and more generalizable than prior work [12] in distilling the underlying semantic representation information over a variety of applications (see Sec. 4.2 and

Sec. 5.1).

Different from previous works, we also exploit the potential of distillation using unlabeled training data often available at scale. This brings together the two fields of knowledge distillation and open-set semi-supervised learning [34], [35], both of which develop independently, and importantly presents a unified perspective and common ground that enable natural model comparison and idea exchange across the two fields.

2.2 Open-Set Semi-Supervised Learning

Most existing semi-supervised learning (SSL) works [36], [37], [38], [39], [40], [41], [42], [43], [44] make a *closed-set* assumption that unlabeled training data share the same label space as the labeled data. This assumption, however, is highly artificial and may hinder the effectiveness of SSL when processing real-world unconstrained unlabeled data with unseen classes, *i.e.*, out-of-distribution (OOD) samples [34]. This is because OOD data could cause harmful error propagation, *e.g.*, via incorrect pseudo labels.

To further generalize SSL to unconstrained data without labels, there is a recent trend of developing more realistic *open-set* SSL methods [35], [45], [46], [47], [48], [49]. A common strategy of these works is to identify and suppress/discard OOD samples as they are considered to be less/not beneficial. Specifically, pioneer methods (UASD [35] and DS³L [45]) leverage a dynamic weighting function based on the OOD likelihood of an unlabeled sample. Curriculum learning has been used to detect and drop potentially detrimental data [46]. Besides, T2T [48] pretrains the feature model with all unlabeled data for improving OOD detection. More recently, OpenMatch [49] trains a set of one-vs-all classifiers for OOD detection and removal during SSL.

Whilst taking a step away from the artificial closed-set assumption, most existing open-set SSL works either focus on a simplified setting where both labeled and unlabeled sets are drawn from a single dataset, or consider only limited known classes and unlabeled data [48], [46] with all the known classes included in the unlabeled set [49], [48]. Clearly, both cases are fairly ideal and hardly valid in many practical cases. To overcome this limitation, we introduce more realistic open-set SSL settings characterized by more classes and unlabeled data with distinct distributions, and less class overlap between labeled and unlabeled sets. Critically, we find that existing open-set SSL methods fail to benefit from using unlabeled data under such unconstrained settings (see Table 11). This challenges all the previous OOD based findings and is thought-provoking. The main reasons we find include more challenging OOD detection and the intrinsic limitation of exploiting unlabeled samples from seen classes alone. Further, our experiments show that knowledge distillation methods provide a more effective and reliable solution to leverage unlabeled data with less constraints (see Table 10 *vs.* Table 11, and Table 14).

3 METHOD

A generic CNN consists of a feature extractor $f : I \rightarrow \mathbf{x}$, and a classifier $h : \mathbf{x} \rightarrow \mathbf{p}$, where $I \in \mathcal{R}^{H \times W \times 3}$, $\mathbf{x} \in \mathcal{R}^d$, $\mathbf{p} = [p_1, \dots, p_k, \dots, p_K] \in \mathcal{R}^K$ denote an input image

sized at $H \times W$, its feature vector of d dimensions, and its classification probability over K classes, respectively. Often, \mathbf{x} is obtained by global average pooling over the last feature map \mathbf{F} . The classifier h is parameterized by a projection matrix $\mathbf{W} \in \mathbb{R}^{d \times K}$ that first projects \mathbf{x} into the logits: $\mathbf{z} = \mathbf{W}^\top \mathbf{x} = [z_1, \dots, z_k, \dots, z_K]$, followed by softmax normalization:

$$p_k = \text{sm}(z_k) = \frac{\exp(z_k)}{\sum_{k'=1}^K \exp(z_{k'})}, \quad (1)$$

where $k \in \{1, \dots, K\}$ indexes the class.

In general *knowledge distillation* [7], we have a teacher network $T = \{f^t, h^t\}$ and a student (target) network $S = \{f^s, h^s\}$. It has two steps in training. In the first step, the teacher network T is pretrained on a labeled training set \mathcal{D}_l in a supervised learning manner. Often, the cross entropy loss is adopted as

$$\mathcal{L}_{ce} = - \sum_{k=1}^K y_k \log p_k \quad (2)$$

where $\mathbf{y} = [y_1, \dots, y_k, \dots, y_K] \in \mathcal{Y}$ is the one-hot ground-truth label of a given input image $I \in \mathcal{D}_l$. In the second step, the student network is then trained under distillation with the frozen teacher and supervised learning with the ground-truth labels (*e.g.*, the cross-entropy loss). A typical knowledge distillation process is realized by logit-matching [7] that minimizes the KL divergence between the logits of T and S as:

$$\mathcal{L}_{kd} = - \sum_{k=1}^K p_k^t \log p_k^s, \quad \text{where } (3)$$

$$\begin{aligned} \mathbf{p}^t &= [p_1^t, \dots, p_K^t] = \text{sm}(\mathbf{z}^t), \mathbf{z}^t = h^t(\mathbf{x}^t), \mathbf{x}^t = f^t(I); \\ \mathbf{p}^s &= [p_1^s, \dots, p_K^s] = \text{sm}(\mathbf{z}^s), \mathbf{z}^s = h^s(\mathbf{x}^s), \mathbf{x}^s = f^s(I). \end{aligned}$$

Whilst this formula has shown to be effective, we consider it is less dedicated on distilling teacher's representation knowledge, especially when considering the structured correlations and inter-dependencies between distinctive feature dimensions.

3.1 Semantic Representational Distillation

To overcome the aforementioned problem, we propose a novel distillation method, dubbed as *Semantic Representational Distillation* (SRD), dedicated to enhancing the representational transfer from the pretrained teacher to the target student in the distillation process. An overview of SRD is depicted in Fig. 1. Specifically, we leverage the pretrained teacher's classifier h^t as a *semantic critic* for explicitly distilling the underlying semantic knowledge of the teacher's representation \mathbf{x}^t to the student's counterpart \mathbf{x}^s . That is, the same classifier is shared by the two representations \mathbf{x}^t and \mathbf{x}^s for facilitating representational knowledge distillation via a dedicated channel.

Formally, we pass the student's representation \mathbf{x}^s through the teacher's classifier h^t to obtain the *cross-network logit* as:

$$\hat{\mathbf{z}} = h^t(\varphi(\mathbf{x}^s)) = [\hat{z}_1, \dots, \hat{z}_k, \dots, \hat{z}_K], \quad (4)$$

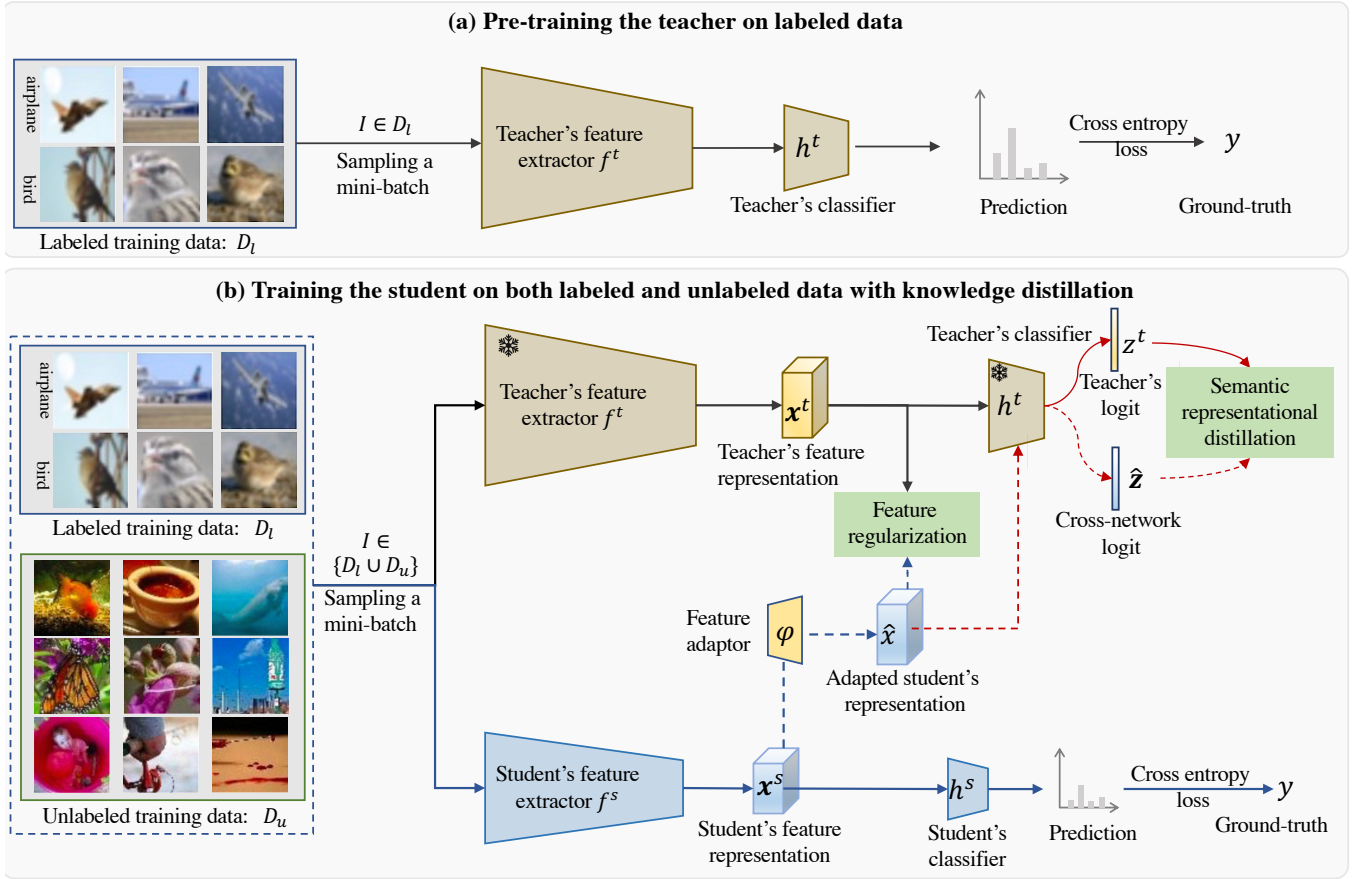


Fig. 1. Schematic overview of the proposed *Semantic Representational Distillation* (SRD) method for knowledge distillation at the presence of both labeled and unlabeled data. Following the knowledge distillation pipeline, (a) we first pretrain a teacher model on the labeled training set. (b) Subsequently, we distil the semantic knowledge from the pretrained frozen teacher to improve the optimization of a student. Specifically, given a training image I , we feed it into both the teacher T and the student S to obtain the feature representations x^t and x^s . Critically, we introduce a notion of *cross-network* logit \hat{z} , obtained by passing the student's representation x^s into the teacher's classifier h^t via a feature adaptor φ . Considering the teacher's classifier h^t as a semantic critic, we distil the semantic knowledge of x^t to x^s via aligning the cross-network logit \hat{z} towards to the teacher's logit z^t . In this design, the two representations x^t and x^s share the same semantic critic (*i.e.*, classifier) which could facilitate representational knowledge distillation. To further ease the semantic distillation, we impose a feature-level alignment regularization \mathcal{R} between the teacher's representation x^t and the adapted student's representation \hat{x} . For labeled training samples, we also apply a supervised learning supervision on the student's prediction.

where φ is a representation adaptor for making x^s compatible with the teacher's classifier. In practice, φ is implemented by a 1×1 convolutional layer with batch normalization and activation applied on the last feature map of the student. We formulate a general SRD objective function as:

$$\mathcal{L}_{srd} = \text{dist}(z^t, \hat{z}), \quad (5)$$

where the teacher's logit z^t , and $\text{dist}(\cdot, \cdot)$ denotes any distance metric. For an extreme case of $z^t = \hat{z}$ (corresponding to the minimal \mathcal{L}_{srd}), since the teacher's classifier is shared by both representations, this means that $x^s = x^t$ subject to some sufficient conditions such as full rank transformation matrix, *i.e.*, the full knowledge of x^t has been transferred to x^s . Generally, minimizing \mathcal{L}_{srd} is equivalent to maximizing the knowledge transfer from x^t to x^s .

SRD objective instantiation: To implement SRD objective, we consider three different designs. The *first* design adopts the KL divergence, following the logit-matching distillation

function as:

$$\mathcal{L}_{srd}^{kl} = - \sum_{k=1}^K p_k^t \log \hat{p}_k, \quad (6)$$

where $\hat{p} = [\hat{p}_1, \dots, \hat{p}_k, \dots, \hat{p}_K] = \text{sm}(\hat{z})$ is the cross-network classification probability and p_k^t is the teacher's classification probability obtained as in Eq. (1). It is noteworthy that, the logit-matching distillation (Eq. (3)) uses specific classifiers h^t/h^s for the representations x^t/x^s , separately; Compared to our SRD sharing a single classifier for both representations, this gives more degrees of freedom to the optimization of feature extractor, resulting in less dedicated constraint on representational knowledge distillation. We will show in the experiments (Sec. 4.1) that our SRD can yield clearly superior generalization capability.

In the *second* design, we adopt the mean square error (MSE) as the distillation loss:

$$\mathcal{L}_{srd}^{mse} = \|z_t - \hat{z}\|^2 = \left\| (W^t)^\top (x^t - \varphi(x^s)) \right\|^2. \quad (7)$$

This is essentially a Mahalanobis distance with the linear transformation defined by the teacher's classifier weights

W^t . As is pretrained, this imposes semantic correlation over all the feature dimensions, making the distillation process class discriminative.

In the *third* design, we consider classification probability MSE by further applying the softmax normalization as:

$$\mathcal{L}_{srd}^{pmse} = \|\mathbf{p}^t - \hat{\mathbf{p}}\|^2. \quad (8)$$

This allows us to evaluate the effect of normalization in comparison to the *second* design. We will evaluate these different designs in our experiment (Table 1).

Overall objective: We formulate the overall loss objective function of SRD on the labeled training set \mathcal{D}_l as:

$$\mathcal{L}_l = \mathcal{L}_{ce}(\mathcal{D}_l) + \alpha\mathcal{L}_{srd}(\mathcal{D}_l) + \beta\mathcal{R}(\mathcal{D}_l), \quad (9)$$

where \mathcal{L}_{ce} is the cross-entropy loss computed between the student’s classification probability \mathbf{p}^s and ground-truth labels, as defined in Eq. (2). $\mathcal{R} = \|\mathbf{x}^t - \varphi(\mathbf{x}^s)\|$ is a feature regularization inspired by the notion of feature matching of FitNets [7]. This is conceptually complementary with SRD loss \mathcal{L}_{srd} as it functions directly in the representation space and potentially facilitates the convergence of our SRD loss. The two scaling parameters α and β control the impact of respective loss terms.

3.2 Meeting Open-Set Semi-Supervised Learning

The aim of knowledge distillation is to transfer the learned knowledge from the teacher to the student. The standard setting is to exclusively use the labeled training set of a *target domain* to train the student. It is a supervised learning scenario. However, distillation methods [7], [11] typically require no ground-truth labels, presenting an unsupervised learning property. Therefore, only using the labeled training set of target domain is unnecessarily restricted and extra unlabeled data should be well incorporated for improved knowledge distillation. Technically, inspired by the spirit of linear algebra, we consider the appearential characteristics of unseen classes can be approximately combined with those of seen classes. In other words, all the seen classes used in our SRD (Eq. (5)) can be viewed *collectively* as a basis of the semantic space including unseen classes.

In light of these above considerations, we further explore the usage of unlabeled data often available at scale in many real-world situations. Typically, there is no guarantee that the unlabeled data only contain the seen/target classes and follow the same distribution as the labeled training set, *i.e.*, *unconstrained unlabeled data with unknown distributions and classes*. This is open-set semi-supervised learning, an emerging problem that has received an increasing amount of attention recently [35], [46], [49], [48]. Under this interesting context of “*Knowledge distillation meets open-set semi-supervised learning*”, we would investigate how knowledge distillation can benefit from unconstrained unlabeled data and previous open-set SSL algorithms, as well as how existing open-set SSL methods can influence the knowledge distillation process.

Formally, except the typical labeled training set \mathcal{D}_l with K known classes \mathcal{Y} as used above, we further exploit an unconstrained set \mathcal{D}_u of unlabeled samples not limited to the same label space \mathcal{Y} . This represents a more realistic

scenario since unlabeled data is typically collected under little or even no constraints, including the set of class labels considered. Our objective is to leverage \mathcal{D}_u for further enhancing the student network on top of \mathcal{D}_l . To that end, we extend the objective function Eq. (9) as:

$$\mathcal{L}_{l+u} = \mathcal{L}_{ce}(\mathcal{D}_l) + \alpha\mathcal{L}_{srd}(\mathcal{D}_l \cup \mathcal{D}_u) + \beta\mathcal{R}(\mathcal{D}_l \cup \mathcal{D}_u), \quad (10)$$

where all the loss terms except the cross-entropy \mathcal{L}_{ce} are applied to \mathcal{D}_u . We summarize our SRD in Algorithm 1.

Remarks: In the open-set SSL literature, the existing methods [35], [46], [49], [48] typically resort to the Out-Of-Distribution (OOD) strategy. The main idea is to identify and discard those samples not belonging to any seen classes of labeled training set (*i.e.*, OOD samples). This is driven by a hypothesis that OOD samples are potentially harmful to SSL. We consider this could be overly restrictive whilst ignoring useful knowledge shared across labeled and unlabeled classes, such as common parts and attributes. For example, flatfish and goldfish exhibit similar body parts such as fins and eyes. Our SRD and other distillation methods can overcome elegantly this limitation by leveraging a pretrained teacher model to extract such information for enhancing the training of a student model. Further, existing open-set SSL works usually consider a small number of unlabelled data with high similarity as labeled data (*e.g.*, object-centric images sampled from the same source dataset). In this paper, we scale this setting by using unconstrained unlabeled data at larger scale and with lower similarity (*e.g.*, scene images). Under such more realistic settings, we reveal new findings in opposite to those reported in previous open-set SSL papers, and show that strategically knowledge distillation is often superior and more reliable than OOD detection in exploiting unconstrained unlabeled data (Sec. 5).

Algorithm 1 Semantic Representational Distillation

Input: A teacher network $T = \{f^t, h^t\}$, a student network $S = \{f^s, h^s\}$, a labeled dataset \mathcal{D}_l , an unlabeled dataset \mathcal{D}_u .

Output: Trained S .

Per-iteration training process:

- 1) Sampling a mini-batch \mathcal{B} from \mathcal{D}_l and \mathcal{D}_u ;
 - 2) Given an image $I \in \mathcal{B}$, feeding it through S to obtain the feature vector \mathbf{x}^s and the logits \mathbf{z}^s ;
 - 3) Similarly, feeding I through T to obtain the feature vector \mathbf{x}^t and the logits \mathbf{z}^t ;
 - 4) Obtaining the cross-network logits (Eq. (4));
 - 5) Computing the objective loss function (Eq. (10));
 - 6) Updating S with SGD.
-

4 KNOWLEDGE DISTILLATION EXPERIMENTS

4.1 Ablation Study

We first ablate SRD on CIFAR-100 [50]. For training, we use SGD with weight decay of $5e-4$ and momentum of 0.9. We set the batch size to 128, the initial learning rate to 0.1 decayed by 0.1 at epochs 100/150 until reaching 200 epochs [30]. We adopt the standard data augmentation scheme [8]

including random cropping (w/ 4-pixels padding) and horizontal flipping. By default, we utilize two variants of Wide ResNet [51], namely WRN40-4 and WRN16-4, as the teacher and student, unless specified otherwise.

SRD loss designs: We first evaluate the three different designs of SRD loss discussed in Sec. 3.1. The corresponding experiments are shown in Table 1 that all these designs are effective with \mathcal{L}_{srd}^{mse} (Eq. (7)) yielding the best results. Interestingly, \mathcal{L}_{srd}^{mse} even slightly surpasses the teacher’s performance. We hypothesize this is due to that our SRD might impose some regularization effect (*e.g.*, fusing the capacity of the student and teacher to some degree) during distillation. Overall, this validates the efficacy of our SRD formulation and loss design. In the following experiments, we hence use \mathcal{L}_{srd}^{mse} as the default design, unless stated otherwise.

TABLE 1

Evaluation of different SRD loss designs on CIFAR-100. Teacher: WRN40-4; Student: WRN16-4.

Accuracy	Top-1 (%)	Top-5 (%)
<i>Supervised learning</i>	76.97	93.89
\mathcal{L}_{srd}^{kl} (Eq. (6))	79.04	95.12
\mathcal{L}_{srd}^{mse} (Eq. (7))	79.58	95.21
\mathcal{L}_{srd}^{pmse} (Eq. (8))	79.13	94.88
Teacher	79.50	94.57

Effect of regularization: Next, we examine the impact of the feature regularization term in Eq. (9). It serves as a feature mimicry constraint to facilitate semantic distillation in the prediction (*e.g.*, logit) space. Table 2 shows that this regularization is useful in improving the semantic distillation, confirming our design choice.

TABLE 2

Effect of feature regularization on CIFAR-100.

Regularization	Top-1 (%)	Top-5 (%)
✗	79.10	94.99
✓	79.58	95.21

Distillation effect: The generic objective of knowledge distillation is to encourage the student mimic the prediction behaviour of the teacher. It is hence insightful to evaluate this mimicry quality. For comparative evaluation, we contrast SRD with the logit-matching distillation [7]. For mimicry measurement, we adopt the KL divergence between the teacher’s and student’s predictions. It is observed from Table 3 that the mimicry ability of a student presents a positive correlation with its accuracy result. That is, more similar to the teacher’s predictions, better model generalization to the test data. Further, we examine qualitatively the feature distribution. It is evident in Fig. 2 that our SRD can better simulate the teacher’s class distribution in the feature space with most of the originally ambiguous boundary regions resolved.

Complementary with logit-matching distillation: We further test the complementary of our SRD with the logit-matching distillation [7]. For extensive evaluation, we experiment with a diverse set of teacher/student pairs using ResNets [52], WRNs [53], MobileNetV2 [54]. Table 4 shows

TABLE 3

Evaluating the distillation effect (*i.e.*, mimicry quality) on CIFAR-100. Metric: KL divergence between the student’s and teacher’s predictions, lower is better.

Method	KL div	Top-1 (%)
<i>Supervised learning</i>	0.5964	76.97
KD [7]	0.5818	78.35
SRD	0.4597	79.58

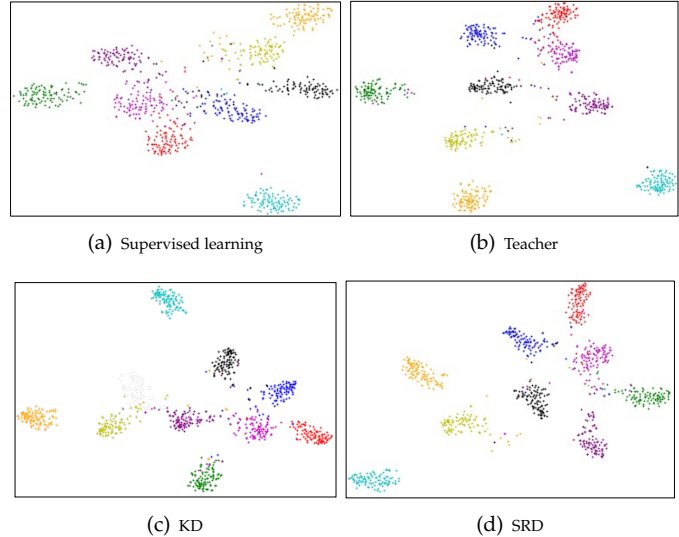


Fig. 2. Feature distribution visualization of 10 classes on CIFAR-100. Class is color coded. Better viewed in color.

that this distillation combination is incompatible and often leads to performance drop in most cases.

TABLE 4

Complementary with logit-matching knowledge distillation [7] on CIFAR-100. Metric: Top-1 accuracy (%). Surp. learn.: Supervised learning.

Teacher (Params)	WRN40-4 (8.97M)	WRN40-4 (8.97M)	ResNet34 (1.39M)	ResNet50 (1.99M)	ResNet34 (21.33M)	WRN40-4 (8.97M)
Student (Params)	WRN16-2 (0.70M)	WRN16-4 (2.77M)	ResNet10 (0.34M)	ResNet18 (0.75M)	WRN16-2 (0.70M)	MobileNetV2 (2.37M)
<i>Surp. learn.</i>	72.70	76.97	68.42	71.07	72.70	68.42
SRD	75.96	79.58	69.91	73.47	75.38	71.82
SRD+KD[7]	74.97	79.00	70.41	73.46	74.90	70.85
Teacher	79.50	79.50	72.05	73.31	78.44	79.50

4.2 Comparison with State-of-the-Art Methods

Architectures: For extensive evaluation, we consider multiple mainstream network architectures including ResNets [52], Wide ResNets [53], MobileNetV2 [54], and MobileNet [55] with different learning capacities.

Competitors: We compare our SRD with five state-of-the-art knowledge distillation methods: KD [7], AT [8], OFD [30], RKD [27], and CRD [12].

Application tasks: Except the common image classification problem, we further consider two more practically critical applications with less investigation in distillation: fine-grained face recognition (Sec. 4.2.4), and binary network optimization (Sec. 4.2.5).

4.2.1 Evaluation on CIFAR-10

Setting: CIFAR-10 is a popular image classification dataset consisting of 50,000 training and 10,000 testing images evenly distributed across 10 object classes. All the images have a resolution of 32×32 in pixel. Following [8], during training, we randomly crop and horizontally flip each image. We train the ResNet for 350 epochs using SGD. We set the initial learning rate to 0.1, gradually reduced by a factor of 10 at epochs 150, 250 and 320. Similarly, we train the WRN models for 200 epochs with the initial learning rate of 0.1 and a decay rate of 5 at epochs 60, 120 and 160. We set the dropout rate to 0. For the logit-matching KD [7], we set $\alpha = 0.9$ and $T = 4$. For AT [8], as in [8], [22], we set the weight of distillation loss to 1000. Note the AT loss is added after each layer group for WRN and the last two groups for ResNet following [8]. Following OFD [30], we set the weight of distillation loss to 10^{-3} . For RKD [27], we set $\beta_1 = 25$ for distance, and $\beta_2 = 50$ for angle, as suggested in [27], [12]. We exclude CRD [12] here because, in our experiments, we found that the parameters originally proposed for CIFAR-100 and ImageNet-1K do not work well for CIFAR-10. We evaluate three types of teacher/student pairs: (1) Two pairs using WRNs; (2) Three pairs using ResNets; (3) One pair across WRN and ResNet.

TABLE 5

Evaluating knowledge distillation methods on CIFAR-10. Metric: Top-1 accuracy (%). The parameter size of each network is given in the round bracket. Surp. learn.: Supervised learning.

Teacher (Params)	WRN16-2 (0.69M)	WRN40-2 (2.2M)	ResNet26 (0.37M)	ResNet26 (0.37M)	ResNet34 (1.4M)	ResNet26 (0.37M)
Student (Params)	WRN16-1 (0.18M)	WRN16-2 (0.69M)	ResNet8 (0.08M)	ResNet14 (0.17M)	ResNet18 (0.7M)	WRN16-1 (0.18M)
Surp. learn.	91.04	93.98	87.78	91.59	93.35	91.04
KD [7]	92.57	94.46	88.75	92.57	93.74	92.42
AT [8]	92.15	94.39	88.15	92.11	93.52	91.32
OFD [30]	92.28	94.30	87.49	92.51	93.80	92.47
RKD [27]	92.51	94.41	88.50	92.36	92.95	92.08
SRD	92.95	94.66	89.02	92.70	93.92	92.94
Teacher	93.98	95.07	93.58	93.58	94.11	93.58

Results: Top-1 classification results on CIFAR-10 are compared in Table 5. On this largely saturated dataset, it is evident that our SRD still results in clear gains over all the alternatives in all settings, suggesting a generic and stable superiority. Besides, it is found that the logit-matching KD performs second only to SRD, surpasses all the other KD variants.

4.2.2 Evaluation on CIFAR-100

Setting: We use the same setting as in ablation (Sec. 4.1). Similarly, we experiment with three sets of teacher/student network pairs. The *first* set is constructed by the performance using WRNs: strong teacher/weak student (WRN40-4/WRN16-2), and strong teacher/fair student (WRN40-4/WRN16-4). The *second* set repeats similar pairings using ResNets: (ResNet34/ResNet10), and (ResNet50/ResNet18). The *third* set is created by combining different architectural families: (ResNet34/WRN16-2) and (WRN40-4/MobileNetV2).

Results: We report the Top-1 performance on CIFAR-100 in Table 6. On this more challenging test, we observe that for almost all teacher/student configurations, our SRD achieves consistent and significant accuracy gains over prior

TABLE 6

Evaluating knowledge distillation methods on CIFAR-100. Metric: Top-1 accuracy (%). Surp. learn.: Supervised learning.

Teacher (Params)	WRN40-4 (8.97M)	WRN40-4 (8.97M)	ResNet34 (1.39M)	ResNet50 (1.99M)	ResNet34 (21.33M)	WRN40-4 (8.97M)
Student (Params)	WRN16-2 (0.70M)	WRN16-4 (2.77M)	ResNet10 (0.34M)	ResNet18 (0.75M)	WRN16-2 (0.70M)	MobileNetV2 (2.37M)
Surp. learn.	72.70	76.97	68.42	71.07	72.70	68.42
KD [7]	74.52	78.35	69.18	73.41	73.95	69.15
AT [8]	74.33	78.06	68.49	71.90	72.32	68.95
OFD [30]	75.57	79.29	68.94	72.79	74.78	70.08
RKD [27]	74.23	78.38	68.70	70.93	73.91	68.19
CRD [12]	75.27	78.83	70.24	73.23	74.88	71.46
SRD	75.96	79.58	69.91	73.47	75.38	71.82
Teacher	79.50	79.50	72.05	73.31	78.44	79.50

methods. Further, there is no clear second best. For WRN pairs, OFD ranks second. For the other cases, CRD instead achieves the second. This suggests that our SRD is also more generalizable to different distillation configurations.

4.2.3 Evaluation on ImageNet-1K

Setting: For larger scale evaluation, we test the standard ImageNet-1K benchmark. We crop the images to a resolution of 224×224 pixels for both training and test. We use SGD with Nesterov momentum set to 0.9, weight decay to 10^{-4} , initial learning rate to 0.2 which decays by a factor of 10 every 30 epochs. We set the batch size to 512. We train a total of 100 epochs for all methods except CRD [12] which uses 10 more epochs following the authors' suggestion. For simplicity, we use pretrained PyTorch models [56] as the teacher [30], [12]. We adopt two common teacher/student pairs: ResNet34/ResNet18 and ResNet50/MobileNet [55]. When testing logit-matching KD [7], we set the weight of KL loss and cross-entropy loss to 0.9 and 0.5, which yields better accuracy as found in [12].

Results: We report the ImageNet classification results in Table 7. Again, we observe that our SRD outperforms all the competitors by a large margin in all cases. This suggests that the advantage of SRD is scalable. Specifically, for the ResNet34/ResNet18 pair, RKD reaches the second best Top-1 accuracy; Whilst in the ResNet-50/MobileNet case, CRD is the second. This further suggests that previous methods are less stable than SRD in the selection of networks. Critically, SRD favors MobileNet with a big margin of absolute 1.1% in absolute terms over the best alternative, CRD. Considering that MobileNet has been widely used across many devices and mobile platforms, this performance gain could be particularly promising and valuable in practice.

4.2.4 Evaluation on face recognition

Except coarse object classification, we also consider fine-grained face recognition task that requires learning more detailed representations specific to individual object instance in the distillation perspective.

Datasets: For training, we use the MS1MV2 dataset [57], a refined version of MS-Celeb-1M [58], [59]. For testing, we use the refined MegaFace [58], [60] which includes a million of distractors. We adopt MegaFace's Challenge1 using FaceScrub as the probe set.

Performance evaluation: We consider two face recognition tasks. (1) *Face verification:* Given a pair of face images, the objective is to determine whether they describe the same

TABLE 7

Evaluating knowledge distillation methods on ImageNet-1K. Metric: Top-1 and Top-5 accuracy (%). The parameter size of each network is given in the round bracket. Surp. learn.: Supervised learning.

Teacher Student	ResNet34 (21.80M)		ResNet50 (25.56M)	
	ResNet18(11.69M)		MobileNet(4.23M)	
	Top-1 (%)	Top-5 (%)	Top-1 (%)	Top-5 (%)
<i>Surp. learn.</i>	70.04	89.48	70.13	89.49
KD [7]	70.68	90.16	70.68	90.30
AT [8]	70.59	89.73	70.72	90.03
OFD [30]	71.08	90.07	71.25	90.34
RKD [27]	71.34	90.37	71.32	90.62
CRD [12]	71.17	90.13	71.40	90.42
SRD	71.73	90.60	72.49	90.92
Teacher	73.31	91.42	76.16	92.86

person’s identity. This is accomplished by calculating a pairwise similarity (e.g., cosine similarity or negative Euclidean distance) in the feature space and matching it *w.r.t.* a threshold. For performance metrics, we adopt the True Acceptance Rate (TAR) at the False Acceptance Rate (FAR) of 10^{-6} [57]. The decision threshold is determined by the FAR. (2) *Face identification*: Given a query face image, the objective is to identify those images with the same person identity in a gallery. This is often treated as a retrieval problem by ranking the gallery images according to the pairwise similarity scores *w.r.t.* the query image. To evaluate the performance, we use the rank-1 accuracy [57].

Competitors: For comparative evaluation, we consider both logit (KD [7]) and feature (AT [8], RKD [27] and PKT [61]) based distillation methods. Note, here we exclude CRD [12] due to its optimization difficulty with margin-based softmax loss and OFD [30] due to its difficulty of finding a good-performing distillation layer.

Setting: For model training, we use SGD as the optimizer and set the momentum to 0.9, and weight decay to $5e - 4$. We set the batch size to 512. We set the initial learning rate to 0.1, and decay it by 0.1 at 100K, and 160K iterations. We train each model for a total of 180K iterations. We adopt ResNet101 [52] as the teacher with 65.12M parameters, and MobileFaceNet [62] as the student with 1.2M parameters.

Results: We present the face recognition results in Table 8. We make several key observations as follows. (1) Our SRD achieves the best distillation in comparison to all the other competing methods, suggesting its superior ability of distilling fine-grained representational knowledge. (2) For face verification, SRD is the only method that improves over the supervised learning baseline, whilst all the others fail. On the contrary, most methods are beneficial for face identification. This may inspire further investigation on fine-grained knowledge distillation in the future. (3) The logit-matching KD [7] fails on both tasks. A plausible reason is due to incompatibility between softened logits matching and margin-based softmax loss. By leveraging the learned identity prototypes with teacher’s classifier to constrain the learning of student’s representation, SRD manages to distil useful knowledge with subtlety successfully.

4.2.5 Evaluation on binary network distillation

In all the above experiments, both student and teacher use some networks parameterized with real-valued precision

TABLE 8

Face identification and verification results on MegaFace. Teacher: ResNet101; Student: MobileFaceNet.

Method	Verification (%)	Identification (%)
<i>Supervised learning</i>	93.44	92.28
KD [7]	92.86	90.91
AT [8]	93.55	92.46
RKD [27]	93.37	92.34
PKT [61]	93.25	92.38
SRD	94.17	93.26
Teacher	98.56	98.82

(real networks). However, they are often less affordable in low-resource regime (e.g., mobile devices). One of the promising approaches is to deploy neural networks with binary-valued parameters (i.e., binary networks, the most extreme case of network quantization), as they are not only smaller in size but run faster and more efficiently [3], [63]. However, training accurate binary networks from scratch is highly challenging and the use of distillation has been shown to be a key component [64]. In light of these observations, we investigate the largely ignored yet practically critical binary network distillation problem. The objective is to distil knowledge from a real teacher to a binary student.

Datasets: In this evaluation, we use CIFAR-100 and ImageNet-1K following the standard setup as above.

Competitors: Similar as face recognition, we compare with both logit (KD [7]) and feature (AT [8], RKD [27], OFD [30], PKT [61], and CRD [12]) based distillation methods.

Setting: For training, we use Adam as the optimizer. For CIFAR-100, we set the initial learning 0.001 decayed by a factor of 0.1 at the epochs of {150, 250, 320} and the total epochs to 350. For ImageNet-1K, we use the initial learning 0.002 decayed by a factor of 0.1 at the epochs of {30, 60, 90}, and a total of 100 epochs. For the teacher and student, we use the same ResNet architecture with the modifications as introduced in [63].

Results: We report binary network distillation results in Table 9. It is evident that on both datasets SRD outperforms consistently all the alternatives by a clear margin. On the other hand, OFD [30] performs worst probably due to its problem specific and less generalizable distillation position. Overall, these results validate that the performance advantage of SRD can extend well from real networks to binary networks, a rarely investigated but practically significant application scenario.

TABLE 9

Binary network distillation results on CIFAR-100 and ImageNet-1K. Metric: Top-1 accuracy (%). Surp. learn.: Supervised learning.

Datasets	CIFAR-100	ImageNet-1K
Teacher	ResNet34(Real)	ResNet18(Real)
Student	ResNet34(Binary)	ResNet18(Binary)
<i>Surp. learn.</i>	65.34	56.70
KD [7]	68.65	57.39
AT [8]	68.54	58.45
OFD [30]	66.84	55.74
RKD [27]	68.61	58.84
CRD [12]	68.78	58.25
SRD	70.50	59.57
Teacher	75.08	70.20

5 OPEN-SET SEMI-SUPERVISED EXPERIMENTS

Datasets In this evaluation, we use *CIFAR-100* [50] as the target dataset, including a labeled training set and a test set. We follow the standard training-test split. To simulate a realistic open-set SSL setting, we use *Tiny-ImageNet* [65] as unlabeled training data. As a subset of ImageNet-1K [66], this dataset consists of 200 classes, each with 500, 50 and 50 images for training, validation and test, respectively. We only use its training set, consisting of 100,000 images. The two datasets share a very small proportion of classes.

Implementation details To facilitate fair comparative evaluation, we adopt the same setup of [12] including the training configuration as given in its open source code¹. For all compared methods below, the same initialization, training and test data are applied under the same training setup. We apply the same data augmentation for all the labeled and unlabeled training data as in Sec. 4.2.2. We resize all the images to 32×32 before data augmentations.

5.1 Evaluation on Knowledge Distillation Methods

Setting We consider a diverse set of three (teacher, student) network pairs for different distillation methods: (ResNet32 \times 4, ResNet8 \times 4), (WRN40-2, WRN40-1), and (ResNet32 \times 4, ShuffleNetV1). For statistical stability, for each experiment we run 5 trials and report the average result.

Competitors We compare extensively a total of 12 state-of-the-art distillation methods: KD [7], FitNet [11], AT [8], SP [22], CC [25], VID [67], RKD [27], PKT [61], AB [29], FT [23], NSP [17], CRD [12]. For all these methods except CRD [12], unlabeled data can be directly accommodated without design adaptation. Instead, class labels are required by CRD [12]. To solve this issue, we extend CRD by a pseudo-labeling strategy. We obtain a pseudo label for every unlabeled sample in a maximum likelihood manner using the teacher network pretrained on the labeled set. We then treat the pseudo labels as the ground-truth during training CRD.

TABLE 10

Comparing distillation methods under the open-set semi-supervised learning setting on CIFAR-100. Labeled training data \mathcal{D} : CIFAR-100; Unlabeled training data \mathcal{U} : Tiny-ImageNet. Metric: Top-1 accuracy (%). The parameter size of each network is given in the round bracket. Supr. learn.: Supervised learning.

Teacher	ResNet32 \times 4 (7.43M)	WRN40-2 (2.25M)	ResNet32 \times 4 (7.43M)			
Student	ResNet8 \times 4 (1.23M)	WRN40-1 (0.57M)	ShuffleNetV1 (0.94M)			
Training data	\mathcal{D}	$\mathcal{D} + \mathcal{U}$	\mathcal{D}	$\mathcal{D} + \mathcal{U}$	\mathcal{D}	$\mathcal{D} + \mathcal{U}$
Supr. learn.	72.50	-	71.98	-	70.59	-
KD [7]	73.33	74.68 \uparrow	73.54	75.08 \uparrow	74.07	76.52 \uparrow
FitNet [11]	73.50	73.30 \downarrow	72.24	71.43 \downarrow	73.59	72.83 \downarrow
AT [8]	73.44	71.75 \downarrow	72.77	73.11 \uparrow	71.73	72.82 \uparrow
SP [22]	72.94	72.10 \downarrow	72.43	73.02 \uparrow	73.48	76.01 \uparrow
CC [25]	72.97	71.96 \downarrow	72.21	70.64 \downarrow	71.14	70.85 \downarrow
VID [67]	73.09	73.48 \uparrow	72.30	73.06 \uparrow	73.38	75.80 \uparrow
RKD [27]	71.90	72.50 \uparrow	72.22	72.99 \uparrow	72.28	73.38 \uparrow
PKT [61]	73.64	75.24 \uparrow	73.45	74.29 \uparrow	74.10	76.50 \uparrow
AB [29]	73.17	72.34 \downarrow	72.38	72.88 \uparrow	73.55	73.33 \downarrow
FT [23]	72.86	71.57 \downarrow	71.59	71.47 \downarrow	71.75	72.81 \uparrow
NSP [17]	73.30	72.06 \downarrow	72.24	72.11 \downarrow	74.12	N/A
CRD [12]	75.51	73.84 \downarrow	74.14	73.54 \downarrow	75.11	76.70 \uparrow
SRD	75.92	76.24\uparrow	74.75	75.32\uparrow	76.40	77.40\uparrow
Teacher	79.42	-	75.61	-	79.42	-

Results We report the results in Table 10. We make the following observations: **(1)** Whilst KD [7], VID [67], RKD [27],

PKD [61], and our SRD consistently improve from using unlabeled training data, FitNet [11] and CC [25] degrade across all different networks. This implies that intermediate feature matching [11] and inter-instance correlation [25] are less robust to unconstrained data. This further verifies that using the high-level feature alignment as in SRD is more reliable. **(2)** Besides, AT [8], SP [22], AB [29], FT [23] and CRD [12] not necessarily improve, conditioned on network pairs. In particular, heterogeneous architectures are preferred by CRD and FT, whilst others present no clear trend. **(3)** Our SRD yields consistently best results, with clear boost up from open-set unlabeled data across all the cases. This suggests the overall performance advantage and network robustness of our model design despite its simplicity. **(4)** Interestingly, the logit-matching KD [7] benefits more from unlabeled data than the other competitors. However, its overall performance is inferior to ours. In a nutshell, this test shows that not all distillation methods can easily benefit from using open-set unlabeled data, with some methods even conditioned on the network choice.

5.2 Evaluation on Semi-Supervised Learning Methods

Setting In addition to distillation methods, we further compare our SRD with existing SSL methods capable of leveraging unlabeled data. To enable comparing the two different approaches, we adopt the same training and test setting as in Sec. 4.2.2. In particular, we adopt the same three student networks as the target models: ResNet8 \times 4, WRN40-1 and ShuffleNetV1. For SRD, we apply the same three (teacher, student) pairs (see top of Table 10). Following the convention of SSL, we report the average result of the last 20 epochs. Note that compared to existing open-set SSL settings [49], [48], [46], our evaluation shares a lower proportion ($\sim 10\%$) of classes between labeled and unlabeled sets and exploits a larger number of both target classes and cross-dataset unlabeled data. For exploring generalization, we will test even less similar unlabeled data (Table 14). This presents a more challenging, realistic, and scalable evaluation scenario.

Competitors We evaluate four representative closed-set (PseudoLabel [37], MeanTeacher [38], MixMatch [39] and FixMatch [36]) and three state-of-the-art open-set (MTCR [46], T2T [48] and OpenMatch [49]) SSL methods. For each method, we adopt its well-tuned default setting provided in the respective source codes. We also include the *supervised learning* baseline without using any unlabeled data.

Results The results are compared in Table 11. We draw several interesting observations. **(1)** With a strong closed-set label space assumption, as expected pseudo labeling [37] gives the poorest performance with significant degradation from the supervised baseline over all three networks. This is because assigning a label for every unlabeled sample in unconstrained open-set setting is highly error-prone. In practice, it is found that $\sim 90\%$ of unlabeled data were wrongly labeled to a single class “*crocodile*” during training and $\sim 50\%$ of test samples were classified as “*crocodile*” mistakenly. **(2)** Relying on less rigid consistency regularization, MeanTeacher [38] yields better performance but still suffers from accuracy drop compared to using only labeled training data. This reveals the limitation of conventional consistency

1. <https://github.com/HobbitLong/RepDistiller>

loss in tackling open-set unlabeled data. (3) Combining consistency regularization and pseudo-labeling, the recent closed-set SSL method FixMatch [36] reasonably performs at a level between [38] and [37]. Note, this is rather different from its original closed-set SSL results, revealing previously unseen limitation of this hybrid strategy. (4) Among all the closed-set SSL methods, MixMatch [39] is the only one capable of achieving accuracy gain from unconstrained unlabeled data. This indicates a new finding that multi-augmentation pooling and sharpening based consistency turns out to be more generalizable to unconstrained open-set SSL. (5) Surprisingly, it is observed that all open-set SSL methods (MTCR [46], T2T [48] and OpenMatch [49]) fail to improve over the supervised learning baseline. This contradicts the reported findings under their simpler and less realistic settings including fewer target classes and unlabeled samples but higher class overlap percentages between labeled and unlabeled sets. This presents a failure case for previous open-set SSL methods and would be thought-provoking and inspire more extensive investigation under more challenging and realistic scenarios with abundant unlabeled data. (6) Our SRD consistently improves the performance of all three networks and surpasses significantly the best competitor MixMatch [39]. This validates a clear advantage of the proposed semantic representational distillation over previous SSL methods in handling open-set unlabeled data. Conceptually, SRD can be also viewed as *semantic consistency regularization* derived from a pre-trained teacher. Our design shares the general consistency regularization spirit whilst differentiating from typical data augmentation based consistency in formulation [39], [36]. (7) Regarding the high-level approach, distillation methods (Table 10) are shown to be generally superior over both closed-set and open-set SSL ones (Table 11). This implies that using a pre-trained teacher model as semantic guidance in various ways could be more advantageous than OOD detection of open-set SSL methods in capitalizing unconstrained unlabeled data. Actually, it is shown that detecting and discarding OOD samples even results in harmful effect over the ignorance of OOD data typical with closed-set SSL methods.

TABLE 11

Comparing state-of-the-art closed-set and open-set semi-supervised learning methods. *Labeled set*: CIFAR-100; *Unlabeled set*: Tiny-ImageNet. *Metric*: Best Top-1 accuracy (%).

Network	ResNet8×4	WRN40-1	ShuffleNetV1
<i>Supervised learning</i>	72.50	71.98	70.50
PseudoLabel [37]	33.33	54.48	42.47
MeanTeacher [38]	70.18	70.25	65.60
FixMatch [36]	68.85	65.54	61.27
MixMatch [39]	<u>74.27</u>	<u>74.01</u>	<u>75.79</u>
MTCR [46]	65.42	61.84	42.34
T2T [48]	66.05	62.55	57.53
OpenMatch [49]	70.41	69.08	66.88
SRD	76.24	75.32	77.40

How does OOD detection fail? To further examine the failure of open-set SSL methods, we analyse the behavior of OOD detection with T2T [48] and OpenMatch [49] during training. In particular, we track the per-epoch proportion of unlabeled data passing through the OOD detector, with

their ground-truth class labels categorized into OOD and in-distribution (IND). It is shown in Fig. 3 that both T2T and OpenMatch can identify the majority of OOD samples at most time whilst keeping away from IND samples at varying rates. However, their performance is still inferior to supervised learning baseline. To further isolate the performance factors, we test particularly the supervised learning component of OpenMatch by deactivating all the unsupervised loss terms. We find that its use of unlabeled data turns out to degrade the performance. This is due to both the challenge of identifying OOD samples under such more difficult open-set settings as studied here, and improper use of unlabeled data. We conjugate that in highly unconstrained open-set SSL scenarios, the OOD strategy has become ineffective. On the contrary, with KD a pre-trained teacher can instead extract more useful latent knowledge (*e.g.*, parts and attributes shared across labeled and unlabeled classes) from unlabeled data not limited to labeled/known classes and more effectively improve the model optimization.

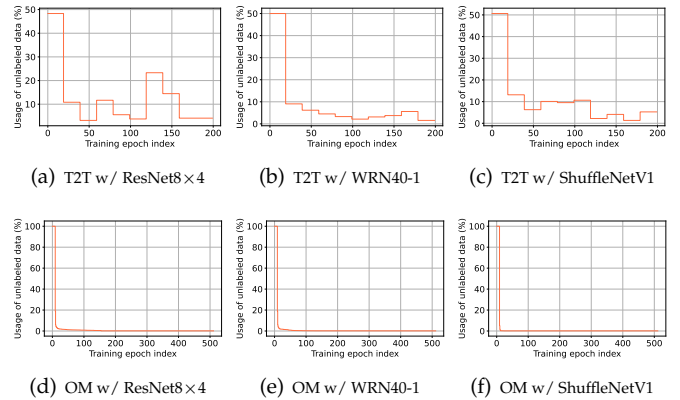


Fig. 3. The per-epoch usage of unlabeled data (those surviving through OOD detection) with (top) T2T [48] and (bottom) OpenMatch (OM) [49].

5.3 Further Analysis

We further analyze a series of unlabeled data and design choices with KD [7] and our SRD in open-set SSL setting.

Effect of unlabeled data size We evaluate the effect of unlabeled data size on the performance. From the training set of Tiny-ImageNet, we create four varying-size ({25%, 50%, 75%, 100%}) unlabeled sets via random and teacher prediction score based selection, respectively. As shown in Fig. 4, both KD and SRD benefit from more unlabeled data regardless of the selection process. This suggests they are generally scalable and insensitive to unlabeled data filtering.

OOD detection It might be interesting to see how OOD works with distillation methods. To that end, we adopt the OOD detector of T2T [48] which is a binary classifier with the teacher’s representation, trained jointly during distillation. It is shown in Table 12 that OOD detection has very marginal effect in most cases, although more unlabeled data on average (Fig. 5) are selected as compared to its original form (Fig. 3). This indicates little complementary between OOD detection and distillation methods.

Data augmentation based consistency A key component with SSL methods is data augmentation based consistency

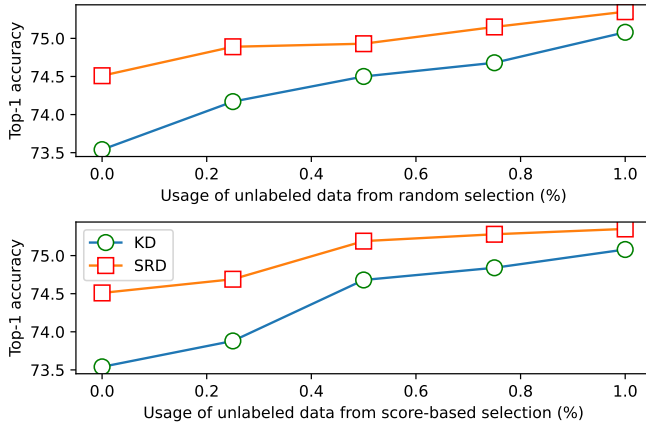


Fig. 4. Size effect of unlabeled data selected (*Top*) randomly or (*Bottom*) by the teacher prediction score. Teacher:WRN40-2. Student:WRN40-1.

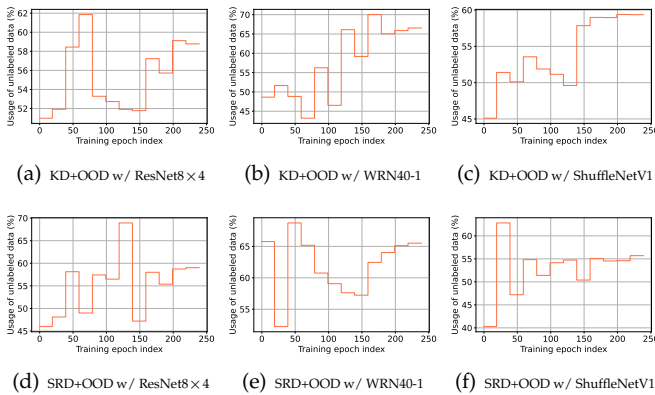


Fig. 5. The per-epoch usage of unlabeled data when an OOD detector is equipped with (*top*) KD [7] and (*bottom*) our SRD.

regularization. Here we examine how it can work together with distillation loss which instead imposes cross-network consistency. We experiment with stochastic augmentation operations including random cropping by up to 4-pixels shifting and random horizon flipping. Given an unlabeled image, we generate two views via data augmentation and feed one view into the teacher and both into the student. A consistency loss is then applied via maximizing their logit similarity. It is shown in Table 13 that data augmentation based consistency would lead to performance degradation. This suggests that cross-network and cross-augmentation consistency are incompatible with each other. As we find, this is because the teacher could output rather different predictions for the two views of a single image (*e.g.*, giving different predicted labels on $\sim 40\%$ of unlabeled images), causing contradictory supervision signal.

More unconstrained unlabeled data For evaluating the generality and scalability in terms of unlabeled data, we test less related unlabeled data by replacing Tiny-ImageNet with *Places365* [68]. This dataset has 1,803,460 training images from 365 scene categories, drastically different from object-centric images from Tiny-ImageNet and CIFAR-100 (see Fig. 6). This hence presents a more challenging open-set SSL scenario. Similarly, we use its training set as unlabeled data. All the other settings remain. We make similar ob-

TABLE 12
Effect of OOD detection on knowledge distillation methods.

Network	ResNet8 \times 4	WRN40-1	ShuffleNetV1
KD [7]	74.68	75.08	76.53
KD+OOD	74.58	75.31	76.54
SRD	76.24	75.32	77.40
SRD+OOD	76.08	75.54	77.41

TABLE 13
Effect of data augmentation based consistency (DAC) on knowledge distillation methods.

Network	ResNet8 \times 4	WRN40-1	ShuffleNetV1
KD [7]	74.68	75.08	76.52
KD [7]+DAC	72.82	74.34	75.64
SRD	76.24	75.32	77.40
SRD+DAC	75.66	73.70	76.34

servations from Table 14. (1) Similarly, all closed-set SSL methods except MixMatch fail to improve over supervised learning baseline. (2) Again, open-set SSL methods are all ineffective and even suffer from more performance drop. (3) Our SRD consistently delivers the best accuracy with a decent margin over the conventional distillation method. (4) Overall, distillation methods remain superior over all SSL competitors, suggesting their generic advantages even at more challenging scenarios with less relevant unlabeled data involved.



Fig. 6. Object-centric images from (a) CIFAR100 and (b) Tiny-ImageNet vs. scene images from (c) Places365 including plate objects.

TABLE 14
Generality and scalability test with further unconstrained unlabeled data from the Places365 dataset.

Network	ResNet8 \times 4	WRN40-1	ShuffleNetV1
<i>Supervised learning</i>	72.50	71.98	70.50
PseudoLabel [37]	21.62	49.96	40.43
MeanTeacher [38]	66.94	53.19	60.32
FixMatch [36]	68.57	66.42	64.26
MixMatch [39]	73.40	73.72	74.89
MTCR [46]	58.08	55.38	33.67
T2T [48]	63.22	61.88	61.54
OpenMatch [49]	58.55	69.80	67.57
KD [7]	74.13	74.29	75.81
SRD	75.93	75.40	77.18

6 CONCLUSION

In this work, we have presented a novel *Semantic Representational Distillation* (SRD) method for structured representational knowledge extraction and transfer. The key idea is

that we take pretrained teacher’s classifier as a semantic critic for inducing a cross-network logit on student’s representation. Considering seen classes as a basis of the semantic space, we further scale SRD to highly unconstrained unlabeled data with arbitrary unseen classes involved. This results in a crossing of knowledge distillation and open-set semi-supervised learning (SSL). Extensive experiments on a wide variety of network architectures and vision applications validate the performance advantages of our SRD over both state-of-the-art distillation and SSL alternatives, often by a large margin. Crucially, we reveal hidden limitations of existing open-set SSL methods in tackling more unconstrained unlabeled data, and suggest a favor of knowledge distillation over our-of-distribution data detection.

REFERENCES

- [1] S. Han, H. Mao, and W. J. Dally, “Deep compression: Compressing deep neural networks with pruning, trained quantization and Huffman coding,” *arXiv*, 2015. [1](#)
- [2] V. Lebedev and V. Lempitsky, “Fast convnets using group-wise brain damage,” in *IEEE Conference on Computer Vision and Pattern Recognition*, 2016. [1](#)
- [3] M. Rastegari, V. Ordonez, J. Redmon, and A. Farhadi, “XNOR-Net: ImageNet classification using binary convolutional neural networks,” in *European Conference on Computer Vision*, 2016. [1](#), [8](#)
- [4] J. Wu, C. Leng, Y. Wang, Q. Hu, and J. Cheng, “Quantized convolutional neural networks for mobile devices,” in *IEEE Conference on Computer Vision and Pattern Recognition*, 2016. [1](#)
- [5] B. Zoph and Q. V. Le, “Neural architecture search with reinforcement learning,” in *International Conference on Learning Representations*, 2017. [1](#)
- [6] H. Liu, K. Simonyan, and Y. Yang, “Darts: Differentiable architecture search,” *International Conference on Learning Representations*, 2019. [1](#)
- [7] G. Hinton, O. Vinyals, and J. Dean, “Distilling the knowledge in a neural network,” *arXiv*, 2015. [1](#), [2](#), [3](#), [5](#), [6](#), [7](#), [8](#), [9](#), [10](#), [11](#)
- [8] S. Zagoruyko and N. Komodakis, “Paying more attention to attention: Improving the performance of convolutional neural networks via attention transfer,” in *International Conference on Learning Representations*, 2017. [1](#), [2](#), [5](#), [6](#), [7](#), [8](#), [9](#)
- [9] S. S. Du and J. D. Lee, “On the power of over-parametrization in neural networks with quadratic activation,” in *International Conference on Machine Learning*, 2018. [1](#)
- [10] M. Soltanolkotabi, A. Javanmard, and J. D. Lee, “Theoretical insights into the optimization landscape of over-parameterized shallow neural networks,” *IEEE Transactions on Information Theory*, 2018. [1](#)
- [11] A. Romero, S. E. Kahou, P. Montréal, Y. Bengio, U. D. Montréal, A. Romero, N. Ballas, S. E. Kahou, A. Chassang, C. Gatta, and Y. Bengio, “Fitnets: Hints for thin deep nets,” in *International Conference on Learning Representations*, 2015. [1](#), [2](#), [5](#), [9](#)
- [12] Y. Tian, D. Krishnan, and P. Isola, “Contrastive representation distillation,” in *International Conference on Learning Representations*, 2020. [1](#), [2](#), [6](#), [7](#), [8](#), [9](#)
- [13] T. Chen, S. Kornblith, M. Norouzi, and G. Hinton, “A simple framework for contrastive learning of visual representations,” in *International Conference on Machine Learning*, 2020. [1](#)
- [14] K. He, H. Fan, Y. Wu, S. Xie, and R. Girshick, “Momentum contrast for unsupervised visual representation learning,” in *IEEE Conference on Computer Vision and Pattern Recognition*, 2020. [1](#)
- [15] T. M. Cover and J. A. Thomas, *Elements of Information Theory (Wiley Series in Telecommunications and Signal Processing)*. USA: Wiley-Interscience, 2006. [1](#)
- [16] J. Yang, B. Martinez, A. Bulat, and G. Tzimiropoulos, “Knowledge distillation via softmax regression representation learning,” in *International Conference on Learning Representations*, 2021. [2](#)
- [17] Z. Huang and N. Wang, “Like what you like: Knowledge distill via neuron selectivity transfer,” *arXiv*, 2017. [2](#), [9](#)
- [18] J. Yim, D. Joo, J. Bae, and J. Kim, “A gift from knowledge distillation: Fast optimization, network minimization and transfer learning,” in *IEEE Conference on Computer Vision and Pattern Recognition*, 2017. [2](#)
- [19] Y. Zhang, T. Xiang, T. M. Hospedales, and H. Lu, “Deep mutual learning,” in *IEEE Conference on Computer Vision and Pattern Recognition*, 2018. [2](#)
- [20] G. Zhou, Y. Fan, R. Cui, W. Bian, X. Zhu, and K. Gai, “Rocket launching: A universal and efficient framework for training well-performing light net,” in *AAAI Conference on Artificial Intelligence*, 2018. [2](#)
- [21] S. H. Lee, D. H. Kim, and B. C. Song, “Self-supervised knowledge distillation using singular value decomposition,” in *European Conference on Computer Vision*, 2018. [2](#)
- [22] F. Tung and G. Mori, “Similarity-preserving knowledge distillation,” in *IEEE International Conference on Computer Vision*, 2019. [2](#), [7](#), [9](#)
- [23] J. Kim, S. Park, and N. Kwak, “Paraphrasing complex network: Network compression via factor transfer,” in *Advances on Neural Information Processing Systems*, 2018. [2](#), [9](#)
- [24] X. Lan, X. Zhu, and S. Gong, “Knowledge distillation by on-the-fly native ensemble,” in *Advances on Neural Information Processing Systems*, 2018. [2](#)
- [25] B. Peng, X. Jin, J. Liu, S. Zhou, Y. Wu, Y. Liu, D. Li, and Z. Zhang, “Correlation congruence for knowledge distillation,” in *IEEE International Conference on Computer Vision*, 2019. [2](#), [9](#)
- [26] J. H. Cho and B. Hariharan, “On the efficacy of knowledge distillation,” in *IEEE International Conference on Computer Vision*, 2019. [2](#)
- [27] W. Park, D. Kim, Y. Lu, and M. Cho, “Relational knowledge distillation,” in *IEEE Conference on Computer Vision and Pattern Recognition*, 2019. [2](#), [6](#), [7](#), [8](#), [9](#)
- [28] Y. Liu, J. Cao, B. Li, C. Yuan, W. Hu, Y. Li, and Y. Duan, “Knowledge distillation via instance relationship graph,” in *IEEE Conference on Computer Vision and Pattern Recognition*, 2019. [2](#)
- [29] B. Heo, M. Lee, S. Yun, and J. Y. Choi, “Knowledge transfer via distillation of activation boundaries formed by hidden neurons,” in *AAAI Conference on Artificial Intelligence*, 2019. [2](#), [9](#)
- [30] B. Heo, J. Kim, S. Yun, H. Park, N. Kwak, and J. Y. Choi, “A comprehensive overhaul of feature distillation,” in *IEEE International Conference on Computer Vision*, 2019. [2](#), [5](#), [6](#), [7](#), [8](#)
- [31] N. Passalis, M. Tzelepi, and A. Tefas, “Heterogeneous knowledge distillation using information flow modeling,” in *IEEE Conference on Computer Vision and Pattern Recognition*, 2020. [2](#)
- [32] H. Jain, S. Gidaris, N. Komodakis, P. Pérez, and M. Cord, “QUEST: Quantized embedding space for transferring knowledge,” in *European Conference on Computer Vision*, 2020. [2](#)
- [33] X. Li, J. Wu, H. Fang, Y. Liao, F. Wang, and C. Qian, “Local correlation consistency for knowledge distillation,” in *European Conference on Computer Vision*, 2020. [2](#)
- [34] A. Oliver, A. Odena, C. A. Raffel, E. D. Cubuk, and I. Goodfellow, “Realistic evaluation of deep semi-supervised learning algorithms,” *Advances in neural information processing systems*, 2018. [3](#)
- [35] Y. Chen, X. Zhu, W. Li, and S. Gong, “Semi-supervised learning under class distribution mismatch,” in *AAAI Conference on Artificial Intelligence*, 2020. [3](#), [5](#)
- [36] K. Sohn, D. Berthelot, N. Carlini, Z. Zhang, H. Zhang, C. A. Raffel, E. D. Cubuk, A. Kurakin, and C.-L. Li, “Fixmatch: Simplifying semi-supervised learning with consistency and confidence,” *Advances in Neural Information Processing Systems*, 2020. [3](#), [9](#), [10](#), [11](#)
- [37] D.-H. Lee, “Pseudo-label: The simple and efficient semi-supervised learning method for deep neural networks,” in *International Conference on Machine Learning Workshop*, 2013. [3](#), [9](#), [10](#), [11](#)
- [38] A. Tarvainen and H. Valpola, “Mean teachers are better role models: Weight-averaged consistency targets improve semi-supervised deep learning results,” in *Advances on Neural Information Processing Systems*, 2017. [3](#), [9](#), [10](#), [11](#)
- [39] D. Berthelot, N. Carlini, I. Goodfellow, N. Papernot, A. Oliver, and C. A. Raffel, “Mixmatch: A holistic approach to semi-supervised learning,” in *Advances on Neural Information Processing Systems*, 2019. [3](#), [9](#), [10](#), [11](#)
- [40] W. Shi, Y. Gong, C. Ding, Z. M. Tao, and N. Zheng, “Transductive semi-supervised deep learning using min-max features,” in *European Conference on Computer Vision*, 2018. [3](#)
- [41] A. Iscen, G. Tolias, Y. Avrithis, and O. Chum, “Label propagation for deep semi-supervised learning,” in *IEEE Conference on Computer Vision and Pattern Recognition*, 2019. [3](#)
- [42] M. Sajjadi, M. Javanmardi, and T. Tasdizen, “Regularization with stochastic transformations and perturbations for deep semi-

- supervised learning," in *Advances on Neural Information Processing Systems*, 2016. 3
- [43] S. Laine and T. Aila, "Temporal ensembling for semi-supervised learning," *International Conference on Learning Representations*, 2017. 3
- [44] T. Miyato, S.-i. Maeda, M. Koyama, and S. Ishii, "Virtual adversarial training: a regularization method for supervised and semi-supervised learning," *IEEE Transactions of Pattern Analysis and Machine Intelligence*, 2018. 3
- [45] L.-Z. Guo, Z.-Y. Zhang, Y. Jiang, Y.-F. Li, and Z.-H. Zhou, "Safe deep semi-supervised learning for unseen-class unlabeled data," in *International Conference on Machine Learning*, 2020. 3
- [46] Q. Yu, D. Ikami, G. Irie, and K. Aizawa, "Multi-task curriculum framework for open-set semi-supervised learning," in *European Conference on Computer Vision*, 2020. 3, 5, 9, 10, 11
- [47] Z. Huang, C. Xue, B. Han, J. Yang, and C. Gong, "Universal semi-supervised learning," in *Thirty-Fifth Conference on Neural Information Processing Systems*, 2021. 3
- [48] J. Huang, C. Fang, W. Chen, Z. Chai, X. Wei, P. Wei, L. Lin, and G. Li, "Trash to treasure: Harvesting OOD data with cross-modal matching for open-set semi-supervised learning," in *IEEE International Conference on Computer Vision*, 2021. 3, 5, 9, 10, 11
- [49] K. Saito, D. Kim, and K. Saenko, "OpenMatch: Open-set consistency regularization for semi-supervised learning with outliers," in *Advances on Neural Information Processing Systems*, 2021. 3, 5, 9, 10, 11
- [50] A. Krizhevsky *et al.*, "Learning multiple layers of features from tiny images," *Tech. Rep.*, 2009. 5, 9
- [51] S. Zagoruyko and N. Komodakis, "Wide residual networks," in *British Machine Vision Conference*, 2016. 6
- [52] K. He, X. Zhang, S. Ren, and J. Sun, "Deep residual learning for image recognition," in *IEEE Conference on Computer Vision and Pattern Recognition*, 2016. 6, 8
- [53] S. Zagoruyko and N. Komodakis, "Wide residual networks," in *British Machine Vision Conference*, 2016. 6
- [54] M. Sandler, A. Howard, M. Zhu, A. Zhmoginov, and L.-C. Chen, "MobileNetV2: Inverted residuals and linear bottlenecks," in *IEEE Conference on Computer Vision and Pattern Recognition*, 2018. 6
- [55] A. G. Howard, M. Zhu, B. Chen, D. Kalenichenko, W. Wang, T. Weyand, M. Andreetto, and H. Adam, "MobileNets: Efficient convolutional neural networks for mobile vision applications," *arXiv*, 2017. 6, 7
- [56] A. Paszke, S. Gross, S. Chintala, G. Chanan, E. Yang, Z. DeVito, Z. Lin, A. Desmaison, L. Antiga, and A. Lerer, "Automatic differentiation in PyTorch," 2017. 7
- [57] J. Deng, J. Guo, N. Xue, and S. Zafeiriou, "Arcface: Additive angular margin loss for deep face recognition," in *IEEE Conference on Computer Vision and Pattern Recognition*, 2019. 7, 8
- [58] Y. Guo, L. Zhang, Y. Hu, X. He, and J. Gao, "Ms-celeb-1m: A dataset and benchmark for large-scale face recognition," in *European Conference on Computer Vision*, 2016. 7
- [59] X. Wu, R. He, Z. Sun, and T. Tan, "A light CNN for deep face representation with noisy labels," *IEEE Transactions on Information Forensics and Security*, 2018. 7
- [60] I. Kemelmacher-Shlizerman, S. M. Seitz, D. Miller, and E. Brossard, "The megaface benchmark: 1 million faces for recognition at scale," in *IEEE Conference on Computer Vision and Pattern Recognition*, 2016. 7
- [61] N. Passalis and A. Tefas, "Learning deep representations with probabilistic knowledge transfer," in *European Conference on Computer Vision*, 2018. 8, 9
- [62] S. Chen, Y. Liu, X. Gao, and Z. Han, "Mobilefacenet: Efficient cnns for accurate real-time face verification on mobile devices," in *Chinese Conference on Biometric Recognition*, 2018. 8
- [63] A. Bulat and G. Tzimiropoulos, "XNOR-Net++: Improved binary neural networks," in *British Machine Vision Conference*, 2019. 8
- [64] B. Martinez, J. Yang, A. Bulat, and G. Tzimiropoulos, "Training binary neural networks with real-to-binary convolutions," in *International Conference on Learning Representations*, 2020. 8
- [65] Y. Le and X. Yang, "Tiny imagenet visual recognition challenge," *CS 231N*, 2015. 9
- [66] O. Russakovsky, J. Deng, H. Su, J. Krause, S. Satheesh, S. Ma, Z. Huang, A. Karpathy, A. Khosla, M. Bernstein, A. C. Berg, and L. Fei-Fei, "Imagenet large scale visual recognition challenge," *International Journal on Computer Vision*, 2015. 9
- [67] S. Ahn, S. X. Hu, A. Damianou, N. D. Lawrence, and Z. Dai, "Variational information distillation for knowledge transfer," in *IEEE Conference on Computer Vision and Pattern Recognition*, 2019. 9
- [68] B. Zhou, A. Lapedriza, A. Khosla, A. Oliva, and A. Torralba, "Places: A 10 million image database for scene recognition," *IEEE Transactions of Pattern Analysis and Machine Intelligence*, 2017. 11